Direct probing of density of states of reduced graphene oxides in a wide voltage range by tunneling junction

Sheng-Tsung Wang,[1] Yen-Fu Lin,[1] Ya-Chi Li,[1] Pei-Ching Yeh,[1] Shiow-Jing Tang,[1] Baruch Rosenstein,[1] Tai-Hsin Hsu,[2] Xufeng Zhou,[3] Zhaoping Liu,[3] Minn-Tsong Lin,[4,5] and Wen-Bin Jian[1]

[1]*Department of Electrophysics, National Chiao Tung University, Hsinchu 30010, Taiwan*
[2]*Energy and Agile System Department, Metal Industries Research and Development Center, Kaohsiung, Taiwan*
[3]*Ningbo Institute of Material Technology and Engineering, Chinese Academy of Sciences, Ningbo, Zhejiang 315201, People's Republic of China*
[4]*Department of Physics, National Taiwan University, Taipei 10617, Taiwan*
[5]*Institute of Atomic and Molecular Sciences, Academia Sinica, Taipei 10617, Taiwan*

(Received 15 September 2012; accepted 17 October 2012; published online 2 November 2012)

Reduced graphene oxide (rGO) sheets are synthesized and tunneling junction devices are fabricated with an aluminum oxide layer inserted in between electrodes and rGO sheets. Differential conductances, revealing density of states (DOS), of rGO sheets are measured in a wide voltage range. A difference in DOS of rGO sheets with different thickness is identified. For the single-layer rGO, the DOS shows a whole band with band edges in line with theoretical predictions, and gating DOS is used to estimate electron's Fermi velocity. Disorder effects on conductance and DOS of rGO sheets are explored and compared with each other. © *2012 American Institute of Physics*. [http://dx.doi.org/10.1063/1.4765361]

The linear energy-momentum dispersion of graphene band structure near the corners of the Brillouin zone was predicted by Wallace in 1946.[1] The theoretical prediction cannot be verified because of the argument about the existence of a truly two-dimensional structure from the thermal-stability consideration. The issue was solved after Novoselov *et al*.[2] demonstrated a metallic electronics of graphene revealing a large electric field effect, in contrast to that in metal films. The result has intensified studies on physics of linear energy-momentum dispersion in graphene and on syntheses of two-dimensional materials.[3–5]

Using angle-resolved photoemission spectroscopy, the linear energy-momentum dispersion near the Dirac point has been directly observed.[6,7] In addition, the band structure and density of states (DOS) of graphene can be probed from differential conductance measurements using scanning tunneling spectroscopy (STS).[8] Though the STS measurement can probe local DOS on graphene surface, a large fluctuation in data owing to tip conditions and tip-to-sample separation discourages its employment in band structure investigations. The technique of tunneling junctions on graphene is developed[9–12] recently to probe the band structure variation.

Previous studies on graphene band structures only focus on a small voltage range near the Dirac point (or Fermi level); thus, it is difficult to catch a complete picture for comparison with the theoretical calculation.[13] Neither can it be used to probe disorder effects,[14] and thickness and stacking dependence of few-layer graphene.[15] In this letter, we characterize electrical properties of reduced graphene oxide (rGO) and applied it to fabrication of tunneling junctions. Through the differential conductance measurements, we will demonstrate a DOS variation of few-layer graphenes with different thickness and a gate voltage dependence of graphene band structure in a wide voltage range.

A soft-chemical exfoliation route was used to prepare graphene oxide flakes.[16] These flakes were chemically reduced and kept in de-ionized water. A substrate of highly doped Si wafer was capped with a 300-nm thick oxide layer and deposited with Ti/Au electrodes of micrometer scale by photolithography patterning. The rGO suspension was drop-casted on the substrate. After dried out, rGO flakes were examined by optical microscope and scanning electron microscope (SEM, JEOL JSM-6700F). Flat flakes with a uniform thickness were selected for device fabrication and the thickness was determined by atomic force microscope (AFM, SII NanoTechnology, SPA-300HV). To improve the conductance, rGO flakes were reduced further by annealing at 400 °C in a high vacuum for 24 h.

Two types of devices, Ohmic-contacted and tunneling-junction devices, were made for probing electron transport and DOS, respectively. For fabrication of Ohmic-contacted devices, two current leads of Ti/Au (10/100 nm in thickness), connecting rGO flakes and pre-patterned electrodes, were made by electron-beam lithography and thermal evaporation. The separation distance between current leads on rGO flakes is about 1 μm. For fabrication of tunneling-junction devices, aluminum oxide (~8 nm in thickness) was deposited on a square area on part of a rGO flake. Two current leads with one on aluminum oxide and the other on rGO flakes were then deposited. These devices were loaded in an insert cryostat (Variable Temperature Insert Cryostat, CRYO Industries of America) in a low vacuum at room temperature or in 1-atm He gas at low temperatures.

Figure 1(a) displays the top view SEM image of a rGO Ohmic-contacted device. The rGO sheet outlined in blue dots is buried under two Ti/Au current leads. Figure 1(b) presents the corresponding diagram of the device and the meter connection. Current-voltage (I-V) curves at varied gate

 © 2012 American Institute of Physics

Downloaded 06 Nov 2012 to 140.112.101.91. Redistribution subject to AIP license or copyright; see http://apl.aip.org/about/rights_and_permissions

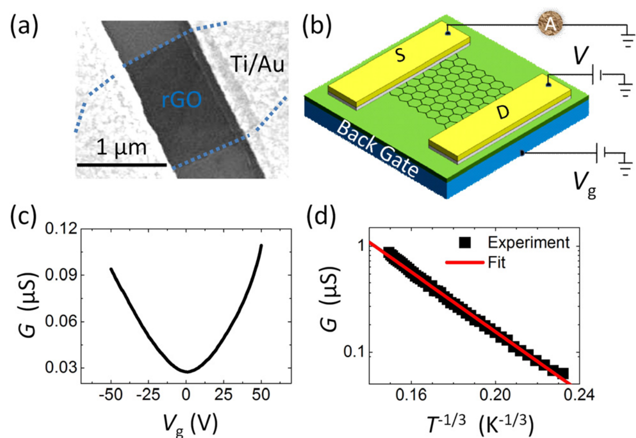

FIG. 1. Transport characterization of rGO sheets. (a) SEM image of a rGO Ohmic-contacted device. (b) Configuration of the conductance measurement. (c) Gate voltage dependence of the rGO conductance at a bias voltage of 0.5 V. (d) Linear dependence of conductance in logarithm scale on $T^{-1/3}$ at temperatures T from 80 to 300 K.

voltage and temperatures are measured and the conductance (G) is evaluated from a linear least square fitting in a small voltage range. The data of gating effect in a voltage rage from −50 to 50 V are shown in Fig. 1(c). The gated conductance reveals a three times of difference in line with the previous report.[17] In comparison with pristine graphene, the smaller electric field effect is owing to an insufficient reduction of graphene oxides. According to the conductivity to reduction-fraction relation,[18] our rGO sheets having conductivities between 10 and 10^3 S cm^{-1} have 20% to 30% of remained graphene oxides. Additionally, Fig. 1(d) exhibits the temperature dependent conductance. The red line in Fig. 1(d) depicts the fitting to the model of the two-dimensional Mott's variable rang hopping of the form $G(T) = G_0 \exp(-(T_0/T)^{1/3})$,[19] where G_0 and T_0 are constants. This result is in line with previous studies of electron transport in rGO.[20]

Figure 2(a) demonstrates the top view SEM image of a rGO tunneling-junction device. The rGO sheet is colored in light gray and outlined in blue dots where one part of the sheet in dark gray is covered by an aluminum oxide layer. Two Ti/Au current leads are deposited with one on the rGO sheet and the other on the oxide layer (see Fig. 2(b)). Here, we introduce a thickness variation thus the topography (AFM image) and the line profile of the thick and thin rGO sheets are offered in Figs. 2(c)–2(f). The thickness of the thick and thin rGO sheets is determined to be ∼3.9 and ∼1.0 nm, respectively. The ∼1.0-nm thick rGO sheet is recognized as a single-layer rGO sheet.[21] Differential conductances (dI/dV) of the thick and the single-layer rGO sheets are plotted in Figs. 2(g) and 2(h). Theoretical calculations of DOS per atom of the single- and the multi-layer graphene[22] do not predict any considerable discrepancies in the window of the whole band width. Nevertheless, our data show a

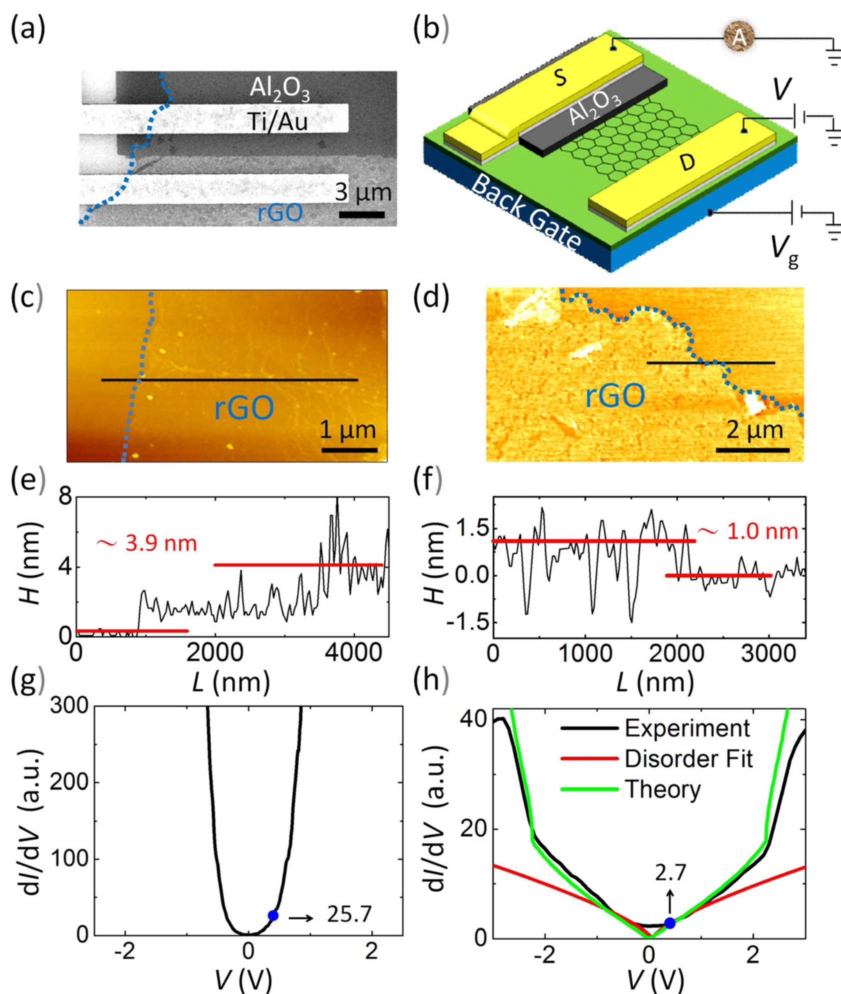

FIG. 2. DOS characterization. SEM image (top view) of a rGO tunneling-junction device (a) and the device configuration with a circuit for the meter connection (b). AFM images of a multi-layer (c) and a single-layer (d) rGO sheet with corresponding line profiles in (e) and (f). Differential conductance (dI/dV) as a function of bias voltage for the multi-layer (g) and the single-layer (h) rGO sheet. The red line in (h) describes a fitting to a power law of V^p with $p \cong 0.66$.

Downloaded 06 Nov 2012 to 140.112.101.91. Redistribution subject to AIP license or copyright; see http://apl.aip.org/about/rights_and_permissions

multiplicative magnitude of DOS in the multi-layer rGO sheet. The multiplication can be rationalized because the DOS of the multi-layer rGO exhibits a summed-up result from each layer's contribution. For example, the dI/dV at 0.4 V are about 25.7 and 2.7 for the multi-layer (Fig. 2(g)) and the single-layer (Fig. 2(h)) rGO sheets that unveil 10 times of variation, which indicates 10 layers of thickness for the multi-layer rGO sheet. Alternatively, the layer number can be estimated from its thickness t of $\sim$3.9 nm by $(t - t_s)/0.34 + 1$, where $t_s \cong 1.0$ nm is the thickness of the single-layer rGO and 0.34 (nm) is the lattice plane spacing;[1] thus, the layer number of 10 is confirmed.

Figure 2(h) signifies a whole band feature of a single-layer rGO that is highly consistent with Robert B. Laughlin's calculations (green line, data reproduced from the plot on his web pages of courses). The steepest ascent around $\pm$3 eV is the band edge, which is very close to the predicted value. An asymmetrical feature on the dI/dV spectrum is commonly observed, signifying a different DOS between empty and filled states. Because we use a rGO sheet rather than a pristine graphene, the disorder effect, causing a nonvanishing differential conductance near the Dirac point and a deviation from a linear energy-momentum relation, shall be considered. We apply a non-linear power law relation $N(E) \sim E^p$,[14] where $N(E)$ is the DOS and $p \leq 1$ is the exponent parameter, to fitting the data in the voltage range between $\pm$0.2V and $\pm$1V. The red line in Fig. 2(h) reveals the fitting result with the estimated p of about 0.66 that manifests the disorder effect in conjunction with a deviation from the linear energy-momentum dispersion.

Figure 3(a) illustrates the gate voltage dependence of the differential conductance of the single-layer rGO sheet. The Dirac point marked by a red arrow shifts from a positive to a negative bias voltage with an increase of the gating voltage. Moreover, the differential conductance distorts severely under a high gating voltage, indicating an electric field effect on DOS. Shifts of the Dirac point are summarized in Fig. 3(b). In our case, if we ignore the disorder amendment of the DOS-energy relation, the Fermi velocity is evaluated to be about 10^7 m/s by the form $E_D = \hbar v_F \sqrt{\pi\alpha|V_g - V_0|}$,[8] where E_D is the shifted energy location of the Dirac point marked in Fig. 3(a), V_g is the gate voltage, and V_0 is the shift of the Dirac point due to intrinsic doping. The estimated Fermi velocity is too high to be true. Considering the disorder effect of the DOS-energy relation and using the revised form of $E_D = \hbar v_F (\pi\alpha|V_g - V_0|)^{1/2p}$, the estimated Fermi velocity of $\sim 4 \times 10^6$ m/s is more close to the ideal value.

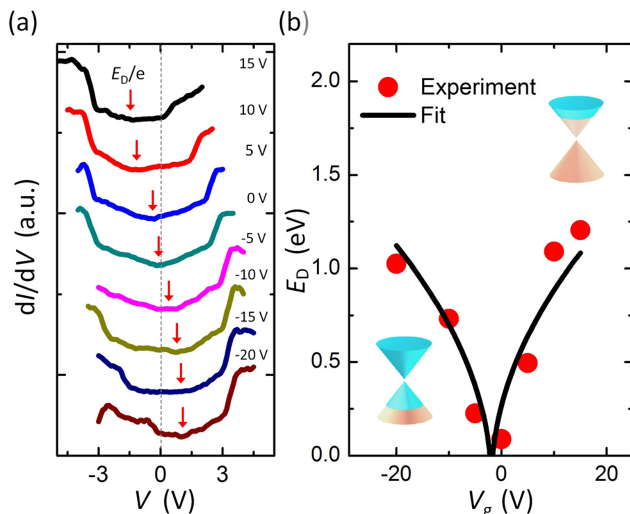

FIG. 3. (a) Gate voltage dependence of differential conductance. (b) Energy position of the Dirac point, extracted from the minimum of the differential conductance in (a), as a function of gate voltage.

The electron transport measurement on rGO sheet shows a hopping conduction and a conductance of several thousand times lower as compared with the pristine graphene. Moreover, it shows a small electric field effect. In contrast, the DOS of the single-layer rGO sheet shows the ideal theoretical prediction of the whole band structure with small deviations of a nonvanishing differential conductance near the Dirac point and a nonlinear DOS-energy relation due to the disorder effect. Even the estimated Fermi velocity is close to the ideal value. These results corroborate that the disorder only makes an increase in electron scattering and a large decrease in electron mean free time but not changes considerably the electronic band structure.

In conclusion, the tunneling junction is made on rGO sheets to perform differential conductance measurements for probing DOS in a wide voltage range. The DOS shows a clear distinction between a single-layer and a multi-layer rGO sheet. For the single-layer rGO sheet, the DOS reveals the whole band structure with a band edge around $\pm$3 eV. The gate voltage dependence of DOS is used to extract the electron's Fermi velocity while the disorder effect needs to be considered. The disorder causes a small modulation of DOS whereas it largely debates the conductance due to electron scattering.

This work was supported by the Taiwan National Science Council under Grant Nos. NSC 98-2112-M-009-013-MY2, NSC 98-2923-M-009-001-MY2, NSC National Nano Project, and by the MOE ATU Program. The authors thank Professor Juhn-Jong Lin for use of his equipment.

[1]P. R. Wallace, Phys. Rev. **71**, 622 (1947).
[2]K. S. Novoselov, A. K. Geim, S. V. Morozov, D. Jiang, Y. Zhang, S. V. Dubonos, I. V. Grigorieva, and A. A. Firsov, Science **306**, 666 (2004).
[3]D. Teweldebrhan, V. Goyal, and A. A. Balandin, Nano Lett. **10**, 1209 (2010).
[4]Md. Z. Hossain, S. L. Rumyantsev, K. M. F. Shahil, D. Teweldebrhan, M. Shur, and A. A. Balandin, ACS Nano **5**, 2657 (2011).
[5]J. Khan, C. M. Nolen, D. Teweldebrhan, D. Wickramaratne, R. K. Lake, and A. A. Balandin, Appl. Phys. Lett. **100**, 043109 (2012).
[6]A. Bostwick, T. Ohta, T. Seyller, K. Horn, and E. Rotenberg, Nat. Phys. **3**, 36 (2007).
[7]M. Sprinkle, D. Siegel, Y. Hu, J. Hicks, A. Tejeda, A. Taleb-Ibrahimi, P. Le Fevre, F. Bertran, S. Vizzini, H. Enriquez *et al.*, Phys. Rev. Lett. **103**, 226803 (2009).
[8]Y. Zhang, V. W. Brar, F. Wang, C. Girit, Y. Yayon, M. Panlasigui, A. Zettl, and M. F. Crommie, Nat. Phys. **4**, 627 (2008).
[9]C. Zeng, M. Wang, Y. Zhou, M. Lang, B. Lian, E. Song, G. Xu, J. Tang, C. Torres, and K. L. Wang, Appl. Phys. Lett. **97**, 032104 (2010).
[10]C. E. Malec and D. Davidović, J. Appl. Phys. **109**, 064507 (2011).
[11]C. E. Malec and D. Davidović, Phys. Rev. B **84**, 121408(R) (2011).
[12]S. Hacohen-Gourgy, I. Diamant, B. Almog, Y. Dubi, and G. Deutscher, Appl. Phys. Lett. **99**, 172108 (2011).
[13]C. Bena and S. A. Kivelson, Phys. Rev. B **72**, 125432 (2005).
[14]K. Ziegler, B. Dóra, and P. Thalmeier, Phys. Rev. B **79**, 235432 (2009).
[15]A. Grüneis, C. Attaccalite, L. Wirtz, H. Shiozawa, R. Saito, T. Pichler, and A. Rubio, Phys. Rev. B **78**, 205425 (2008).
[16]X. Zhou and Z. Liu, Chem. Commun. **46**, 2611 (2010).

Downloaded 06 Nov 2012 to 140.112.101.91. Redistribution subject to AIP license or copyright; see http://apl.aip.org/about/rights_and_permissions

[17]X. Dong, C. Y. Su, W. Zhang, J. Zhao, Q. Ling, W. Huang, P. Chen, and L. J. Li, Phys. Chem. Chem. Phys. **12**, 2164 (2010).
[18]C. Mattevi, G. Eda, S. Agnoli, S. Miller, K. A. Mkhoyan, O. Celik, D. Mastrogiovanni, G. Granozzi, E. Garfunkel, and M. Chhowalla, Adv. Funct. Mater. **19**, 2577 (2009).
[19]N. F. Mott, *Conduction in Non-Crystalline Materials* (Clarendon, Oxford, 1993).
[20]C. Gómez-Navarro, R. T. Weitz, A. M. Bittner, M. Scolari, A. Mews, M. Burghard, and K. Kern, Nano Lett. **7**, 3499 (2007).
[21]S. Stankovich, D. A. Dikin, G. H. B. Dommett, K. M. Kohlhaas, E. J. Zimney, E. A. Stach, R. D. Piner, S. T. Nguyen, and R. S. Ruoff, Nature **442**, 282 (2006).
[22]C. L. Lu, C. P. Chang, Y. C. Huang, J. M. Lu, C. C. Hwang, and M. F. Lin, J. Phys.:Condens. Matter **18**, 5849 (2006).

Downloaded 06 Nov 2012 to 140.112.101.91. Redistribution subject to AIP license or copyright; see http://apl.aip.org/about/rights_and_permissions